Korean J. Chem. Eng., 40(11), 2744-2750 (2023)
DOI: 10.1007/s11814-023-1479-y

pISSN: 0256-1115
eISSN: 1975-7220

Fabrication of g-C_3N_4 nanosheets on stainless steel mesh for effective separation of oil from water

Nada Saeed Al-Kindi[*,], Faisal Al Marzouqi[***], Majeda Khraisheh[****], Younghun Kim[*****,†], and Rengaraj Selvaraj[*,†]**

*Department of Chemistry, College of Science, Sultan Qaboos University, P. O. Box 36, P.C. 123, Al-Khoudh, Muscat, Sultanate of Oman
**Department of Applied Sciences, University of Technology and Applied Science, Alkuwair 133, Muscat, P. O. 74, Sultanate of Oman
***Department of Engineering, International Maritime College Oman, National University, P. O. Box: 532, PC: 322, Falaj Al Qabail, Suhar, Sultanate of Oman
****Department of Chemical Engineering, College of Engineering, Qatar University, Doha P. O. Box 2713, Qatar
*****Department of Chemical Engineering, Kwangwoon University, Seoul 01891, Korea
(*Received 20 February 2023 • Revised 1 April 2023 • Accepted 1 May 2023*)

Abstract−Most industries depend mainly on oil and oil-based processes, which resulted in producing large volumes of oily wastewater. One of the most common methods used for the treatment of oily contaminated water is filtration by modified surfaces. In this research g-C_3N_4 nanostructured material was prepared via thermal condensation method. The samples were characterized by advanced techniques such as XRD, XPS, FTIR scanning electron microscopy (FE-SEM) and energy dispersive X-ray spectrophotometry (EDX). The result showed that g-C_3N_4 were crystallized in tri-s-triazine phases and their mean crystalline sizes of these nanostructures were 12.17 nm. The high-magnification microscopy images show that the morphology of g-C_3N_4 was nanosheet. A stainless-steel mesh was modified and coated with the prepared g-C_3N_4 nanostructured materials to be used for the separation of oil and water mixture. Due to the hydrophobic nature of the modified meshes, oil drops spread over the mesh surface and the water drops form spherical shapes. The most efficient coating among all the modified meshes was g-C_3N_4, which was functionalized using silane moiety. The separation efficiency of this coated mesh reached 74.87% and it resulted in fast separation. This mesh can separate different types of oil from the oil/water mixture, such as toluene, mineral oil, 2-ethyl-1-hexanol, and n-pentane with good efficiency. Separation was repeated up to 40 times using the same mesh, and the separation efficiency was measured each time.

Keywords: Oil-water Separation, Oily Wastewater, Mesh, g-C_3N_4

INTRODUCTION

A large amount of oily wastewater is produced by different industries, which increases the probability of oil leakage during transportation in the ocean. As a result, oily wastewater is considered one of the common wastes all over the world. To solve this problem, a superhydrophobic material is considered as best candidate among other materials, and this is a clear indication of the researchers' interest in the last years [1-3]. In the literature, metal meshes and sponges were modified using different methods to be used for oil\water separation [4].

Stainless-steel mesh with 75 μm size mesh was used and coated with cerium (IV) oxide (CeO_2) nanoparticles using the spray coating method [5]. The efficiency of the coated mesh, gravity-driven filtration was carried without any additional energy or force. The obtained separation results prove the hydrophobicity of the coated mesh by allowing the oil to pass through the mesh and the water was left behind [6,7]. Coated copper mesh with CuS and Cu_2S micro-particles using the hydrothermal method were water contact angle (CA) was measured to investigate the nature of the coated mesh (CA=160°). A research group succeeded to modify superhydrophobic stainless-steel mesh coated with ZnO particles using chemical immersion growth. The ZnO coated mesh shows high separation efficiency for all the oil\water mixtures [8]. Furthermore, it maintains high separation efficiency even after repeating the separation ten times. The CA of water and oil obtained from the surface wettability analysis was 122° and 0°, respectively. This indicates the complete spreading of oil and the hydrophobic nature of the mesh, which results in keeping the water droplets as spheres in the modified mesh surface [9]. Similarly, highly efficient superhydrophobic copper meshes, which were coated with hierarchical micro-structured polyimide layer modified by lauroyl groups to be used for the separation of oil/water mixtures. The long alkyl chains of the coating material and the water contact angle of the mesh surface (CA> 150°) were the main reasons for the superhydrophobic and superoleophilic properties of the mesh [10].

†To whom correspondence should be addressed.
E-mail: korea1@kw.ac.kr, rengaraj@squ.edu.om

Different oils were used to be separated from water such as isooctane, petroleum ether, n-hexadecane, and chloroform. All the oil\water mixtures were separated using a modified mesh with high separation efficiency (above 95%) [11,12]. After repeating the separation of chloroform/water mixture using the modified mesh up to 20 times, the separation efficiency was still above 99%, and this indicates the chemical durability of the coating method [2]. A one-step spray of polyurethane and hydrophobic silica nanoparticles was used to develop water-repellent superhydrophobic copper mesh.

The modified mesh has many properties, such as good recyclability, high absorption capacity, and it can separate the oil/water mixture with a temperature of 100 °C. A stainless steel mesh with TiO_2 nanomaterial was one of photocatalysts, using the fast dip-coating method. The oil\water separation was performed by gravity-driven filtration using the TiO_2 coated mesh. The separation was very fast (3 s) and high efficient (98-99%) even after 20 recycles [13].

Recently, carbon based photocatalysts have emerged as promising conducting materials due to their high chemical and thermal stability. Carbon nitride (g-C_3N_4) is an interesting 2D material. A great deal of attention has focused on the use of g-C_3N_4 for pollutant degradation and chemical synthesis [14,15]. Herein, the research investigated the modification of stainless steel mesh with carbon nitride material for separation of water from oily contaminated water. Two main nitrogen rich carbon materials were used and different tests were performed to investigate the nature of the coated meshes and their stability and efficiency. In this work, the nanostructured materials prepared are graphitic carbon nitride (g-C_3N_4) from different precursors. As-prepared g-C_3N_4 was immobilized on the stainless steel mesh to use as oil\water separating filter.

EXPERIMENTAL

1. Materials

The precursors used in the preparation of graphitic carbon nitride (g-C_3N_4) nanostructured material were melamine and thiosemicarbazide. Stainless-steel meshes (SUS 304, Eulji-steel) with different mesh sizes (50, 75, 100, 150, and 300 μm) were the main substrate and the synthesized nanostructured materials were coated on its surfaces. Sodium hypophosphite hydrate and 1,2,3,4-butanetetracarboxylic acid (BTCA) were used to prepare the binding agent solution. Hexadecyltrimethoxysilane (HDTMS), (3-aminopropyl)-triethoxysilane (APTES), dichlorodimethylsilane (DCDMS), and chlorotrimethylsilane (CTMS) were used as hydrophobic agents.

2. Synthesis of g-C_3N_4 Using Different Precursors

The g-C_3N_4 was synthesized in a muffle furnace using the thermal condensation method. 1 g of each precursor (melamine, and thiosemicarbazide) was weighed using an analytical balance and placed into crucibles and covered tightly with a lid. Then, the crucibles were subjected to direct heating by increasing the temperature to 550 °C at a heating rate of 3 °C/min and held for 12 h and 3 h for melamine and thiosemicarbazide, respectively [16-18]. After cooling, the product was ground into powder and collected for further analysis. Melamine results in yellow g-C_3N_4 nanostructures, while thiosemicarbazide gives intense yellow solid.

3. Optimization of Mesh Coating

The dimension of the mesh used was 5×5 cm^2. The pre-treatment of the mesh started by cleaning it using acetone. After the complete drying of the mesh, further cleaning was performed using an acid solution. The mesh was immersed in a cleaning solution containing sulfuric acid and sodium dichromate at 60 °C for 1 h. This acid treatment helps to make the mesh surface rough, and it causes mesh etching. Thereafter, the clean mesh was dipped in the binding agent solution at 50 °C for 1 h. The binding agent solution is a mixture of BTCA and sodium hypophosphite hydrate in distilled water. After the complete drying of the mesh, it was immersed in the coating solution for 1 h, which contains 1 g from any of the prepared nanostructured material (g-C_3N_4) suspended in ethanol (100 mL). Next, the nanostructured material in the mesh surface was functionalized by dipping the mesh in the hydrophobic agent solution for 1 h. This solution was prepared from 4 wt% of any hydrophobic silane agent (HDTMS, APTES, DCDMS, and CTMS) dissolved in ethanol. Finally, the modified mesh was subjected to heat treatment in the oven (120 °C) for 1 h. This step makes the mesh surface more mechanically robust.

4. Oil/Water Separation

After the stainless-steel meshes (with different mesh sizes) were coated with nanostructured materials using the optimized method, the separation ability of the meshes was tested. Distilled water was colored using methylene blue (blue color), while the oil (toluene, hexane, mineral oil, 2-ethyl-1-hexanol, and n-pentane) was colored using Sudan red III (red color). Different tests were performed to investigate the properties of the coated mesh (hydrophobic or hydrophilic). The mesh was folded as a boat shape and the colored oil/water mixture was poured through the mesh (without vacuum or pressure). The separation efficiency was calculated by weighing the oil mass before and after the separation process. To test the repeatability and the stability of the coated mesh, the separation was repeated several times (up to 20 times and even more).

5. Characterization

The crystalline and the structural properties were studied by X-ray diffraction analysis (XRD) using a bench top X-ray diffractometer (X'Pert Pro). The chemical states and the elemental composition were measured using multi-probe X-ray photoelectron spectroscopy (XPS) (Scienta Omicron). Fourier transform infrared spectra (FTIR) were recorded using FTIR spectrophotometer (ALPHA II, Bruker). The morphological features were examined by field-emission scanning electron microscopy (FE-SEM) (JSM-7600F, Jeol. The ratio of the elements within the surface was identified using an energy dispersive X-ray spectrophotometer (EDX) equipped with FE-SEM.

RESULTS AND DISCUSSION

1. Characterization of g-C_3N_4

As-prepared nanostructured materials were characterized via XRD technique to investigate the structural and crystalline properties, such as crystal structure, crystal quality, and mean grain size. Fig. 1 shows both the XRD patterns could be indexed to the tri-s-triazine structure of g-C_3N_4 (JCPDS No. 87-1526). The typical peaks of g-C_3N_4 were observed at 2θ values of 13.8° and 27.8° correspond to (100) and (002) reflection planes, respectively [16]. The strongest XRD peak, which is indexed for the lattice plane of (002), is

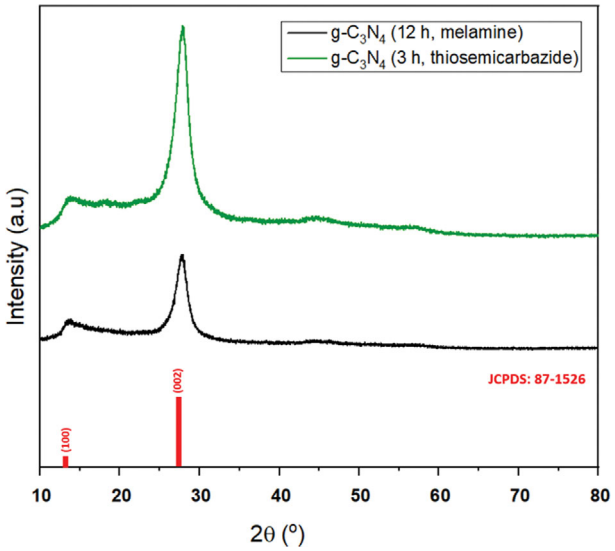

Fig. 1. XRD patterns of g-C_3N_4 samples prepared using different precursors.

due to the inter-planar stacking of the conjugated aromatic system in the tri-s-triazine building units, where the electron has stronger inter-layer binding. The XRD patterns obtained for g-C_3N_4 samples are widely accepted as the g-C_3N_4 tri-s-triazine building block [17,18]. The mean grain size of both samples is approximately 12.1 nm, which was calculated with Debye-Scherrer's equation. It means that crystalline structure of g-C_3N_4 was not affected by precursor type.

To investigate the chemical composition of g-C_3N_4 synthesized by the thermal condensation of precursors, X-ray photoelectron spectroscopy (XPS) was performed (Fig. 2). In the XPS survey spectrum, shown in Fig. 2(a), three peaks were observed, which indicate that the synthesized material is composed of primarily carbon and nitrogen; however, a small amount of oxygen was also detected. The oxygen came from surface absorption and oxidation. Two peaks are shown in the high-resolution spectrum of C1s at the positions of 288.18 eV and 284.68 eV (Fig. 2(b)). The peak observed at 284.68 eV is absolutely assigned to (C-C bonding) in a pure carbon environment. Whereas the broad peak at 288.18 eV is attributed to carbon atoms bonded with three N neighbors. On the other hand, the XPS spectrum of N1s shows two main peaks (Fig. 2(c)). The broad peak could be deconvoluted into two peaks with binding energies of 398.64 eV and 400.05 eV. The peak at 398.64 eV corresponds to sp^2 N atoms in the triazine rings, while the other peak is attributed to N atoms in N-$(C)_3$. The additional weak peak

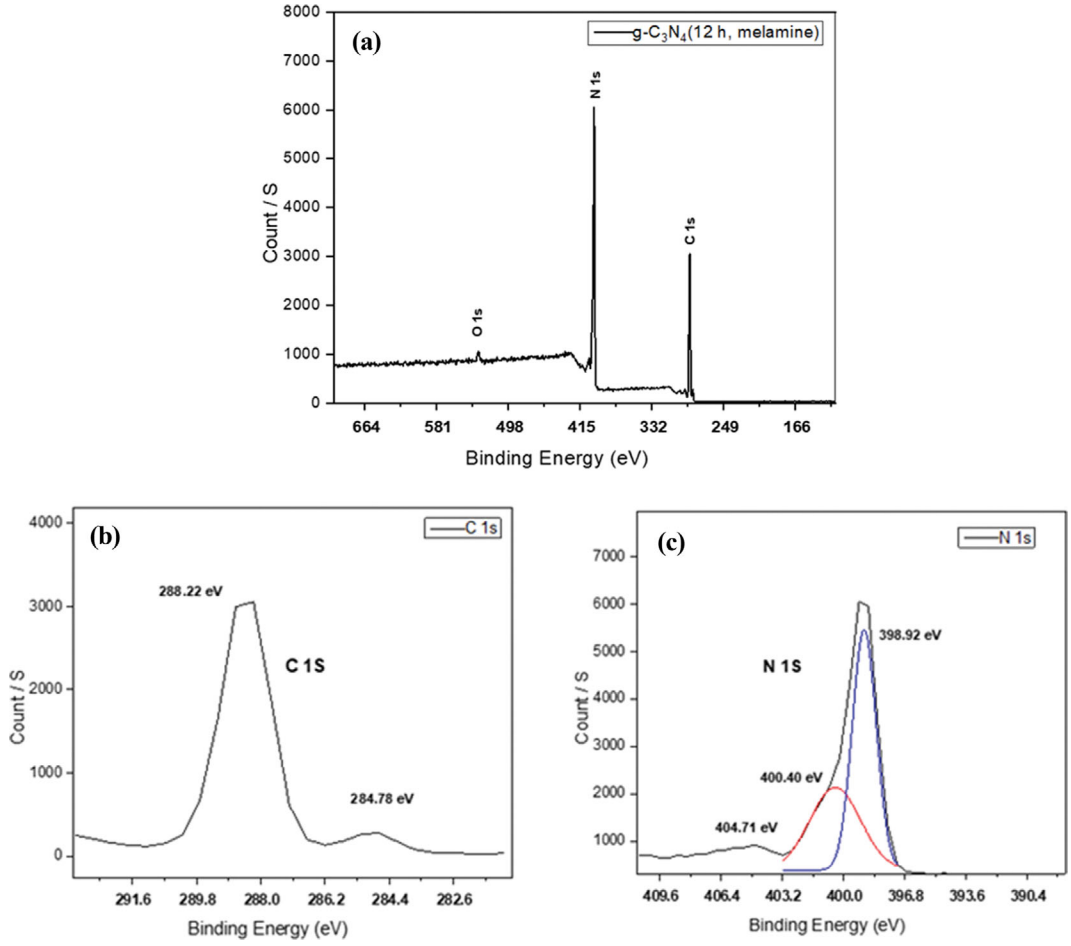

Fig. 2. (a) XPS survey spectrum of g-C_3N_4 synthesized from melamine (b) High-resolution XPS spectrum of C 1s and (c) N 1s peaks.

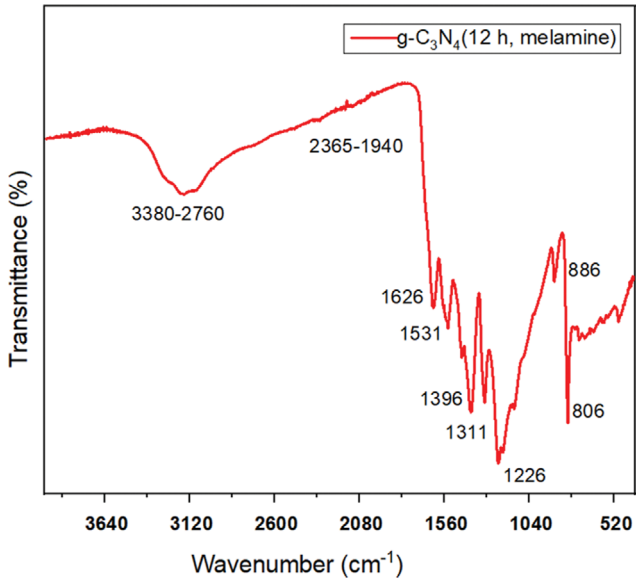

Fig. 3. Room temperature FTIR spectrum of g-C_3N_4 synthesized from melamine.

at 404.39 eV is ascribed to the -NH_2 or NH groups. The obtained XPS data of g-C_3N_4 are strongly agreed with the literature [16,19, 20].

Fig. 3 depicts the typical FTIR spectrum of g-C_3N_4 obtained by heating melamine. The spectrum shows a broad band corresponding to the stretching and deformation modes of the -NH and NH_2 group (and possibly OH) at 2,760-3,380 cm^{-1} (centered at 3,160 cm^{-1}). Meanwhile, a weak band at 886 cm^{-1} of the deformation mode of N-H is present. In addition, the low intense peaks at 1,940-2,365 cm^{-1} may be due to the stretching of the C≡N group. The peak at 1,626 cm^{-1} characterizes the C=N stretching modes, whereas the peaks at 1,311 cm^{-1} and 1,226 cm^{-1} characterize the C-N stretching. Furthermore, a group of multiple bands characteristic for tri-s-triazine ring vibrations were observed at 1,531 cm^{-1}, 1,396 cm^{-1}, and 806 cm^{-1}. It is known in the literature that the peak at 1,531 cm^{-1} is an indication of good crystallinity of the synthesized g-C_3N_4 [14,15,17].

The morphological features of the synthesized nanostructured materials were examined via SEM. Fig. 4 shows the low-magnification SEM images of g-C_3N_4 synthesized from different precursors using the thermal condensation method. Both images show the same morphology, which is composed of a large number of soft and fluffy nanosheets with irregular laminated structures.

2. Coating of g-C_3N_3 on Mesh and Oil\Water Separation

In this research, stainless-steel meshes with different mesh sizes were used as a substrate to be modified for oil/water separation. Fig. 5(a) shows the surface morphology of the stainless-steel meshes after being coated with g-C_3N_4. As it is obvious from the SEM images, a layer of the nanostructured material is introduced on the smooth surface of the stainless-steel mesh. Moreover, the clustered structures of the nanomaterials are randomly distributed in the stainless-steel mesh. Figs. 5(b)-(d) show the EDX data of mesh coated with g-C_3N_4. To investigate the hydrophobicity of surface, CA value of the coated meshes was measure, as given in Table 1. Except APTES, CA of g-C_3N_4 coated mesh was larger than 110°. This means that the surface of the coated meshes is not wettable or hydrophobic, so it will not allow the water to pass through. CA of 75 μm mesh was slightly larger than that of 50 μm mesh.

The separation efficiency is measuring the ability of the mesh to separate oil from water in the oil/water mixture. To study the effect of coating in general, the separation was performed using uncoated meshes with different mesh sizes. All the uncoated meshes allow the passage of both water and oil, resulting in inefficient separation. The step after choosing the most efficient mesh sizes (50 μm and 75 μm) is to find the most suitable hydrophobic agent for the separation. The small size has more surface material, all more attachment with hydrophobic agent and nanomaterial. As shown in Table 1, different meshes coated with g-C_3N_4 were functionalized with different hydrophobic agents, and the separation efficiency was measured. From the obtained results, the meshes coated with HDTMS give the highest efficiency, which means it is more suitable for separation. The long carbon chain in HDTMS resulted in to increase in the hydrophobicity of this agent which makes it more efficient in the separation process.

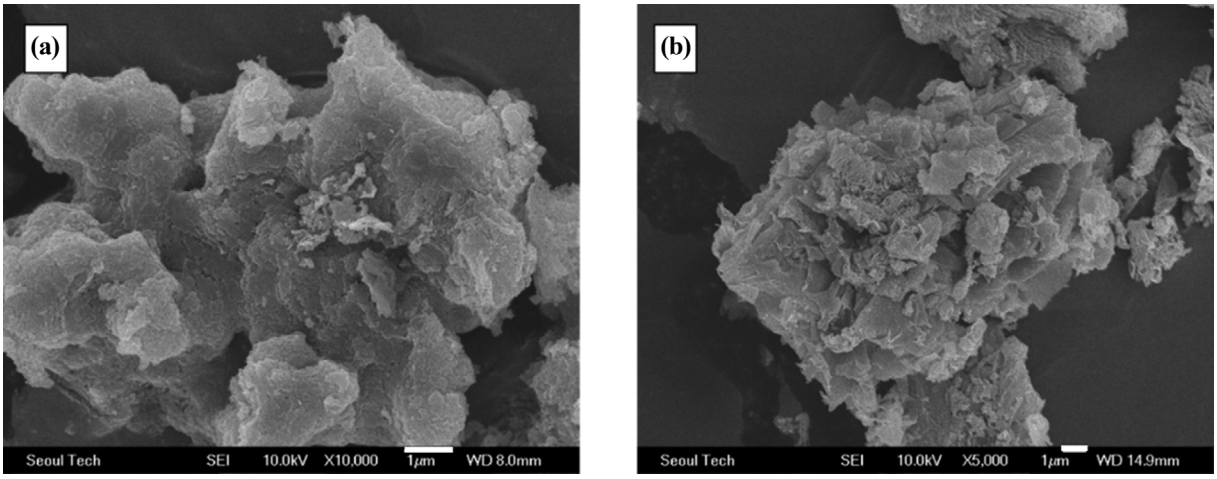

Fig. 4. SEM images of g-C_3N_4 synthesized from (a) thiosemicarbazide, and (b) melamine.

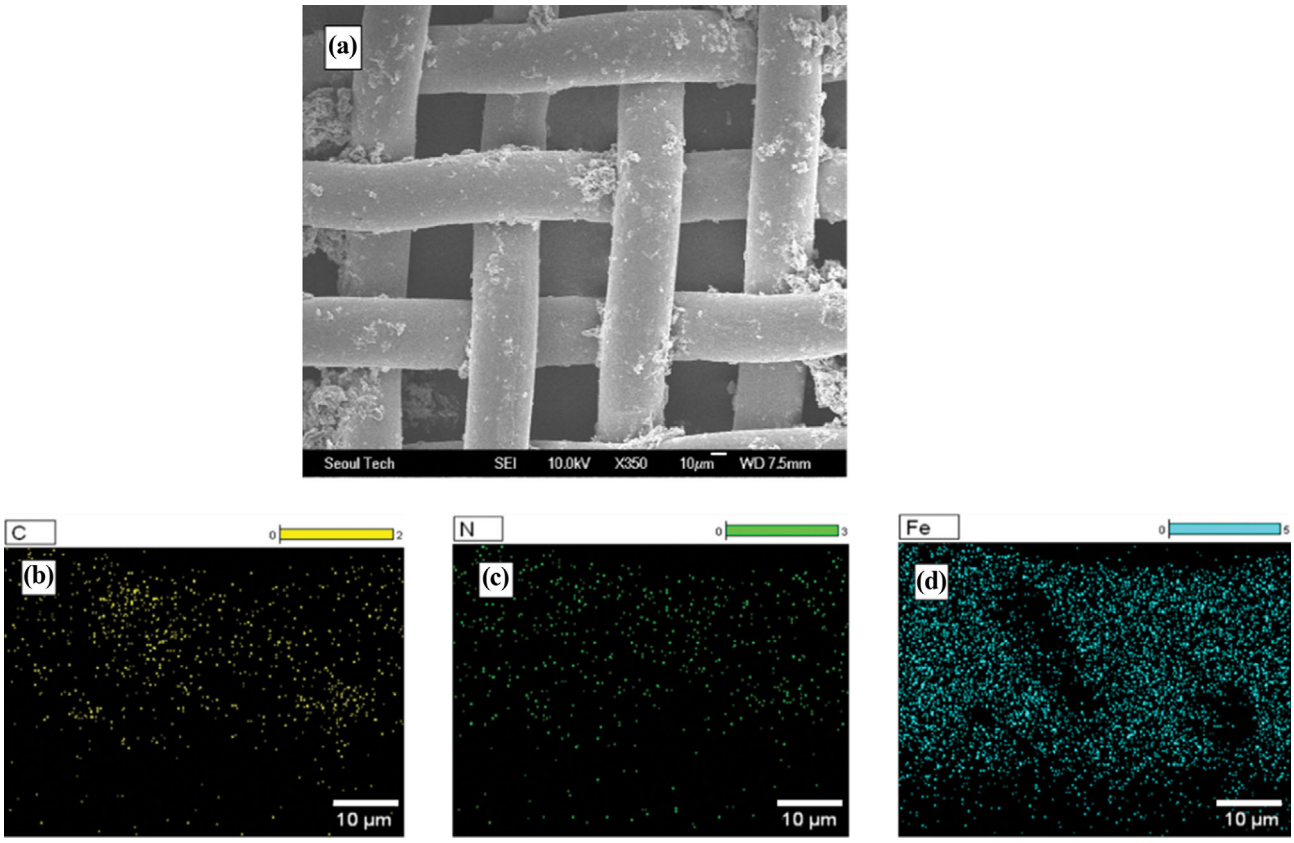

Fig. 5. (a) SEM image and (b)-(d) EDX elemental mapping images of stainless-steel mesh coated with g-C_3N_4 synthesized from melamine.

Table 1. CA value and separation efficiency of g-C_3N_4 coated meshes

Stainless-steel mesh			CA	Separation efficiency
Mesh type	Mesh size	Hydrophobic agent		
Uncoated	50 μm	-	64.45°	-
	75 μm		85.72°	
	100 μm		82.39°	
	150 μm		75.12°	
	300 μm		68.29°	
Coated with g-C_3N_4 (melamine)	50 μm	HDTMS	114.80°	71.75%
	75 μm		127.25°	73.40%
	50 μm	APTES	56.36°	67.31%
	75 μm		62.76°	69.81%
	50 μm	DCDMS	120.41°	64.10%
	75 μm		125.54°	68.91%
	50 μm	CTMS	118.15°	62.16%
	75 μm		115.14°	65.96%
Coated with g-C_3N_4 (thiosemicarbazide)	50 μm	HDTMS	128.55°	70.46%
	75 μm		133.47°	74.87%

From the previous tests, the separation efficiency of stainless-steel meshes coated with different nanostructured materials was measured . As obvious from the separation efficiency results in the table, the mesh coated with g-C_3N_4 synthesized from thiosemicarbazide gives the highest efficiency (74.87%). The high efficiency of the g-C_3N_4 coating is due to the morphology of the carbon nitride, which forms as nanosheets [16]. This shape resulted in a good coating of the stainless-steel mesh surface. The most efficient mesh (g-C_3N_4 coated mesh functionalized with HDTMS –75 μm) was used for further tests such as repeatability, stability, and accuracy test.

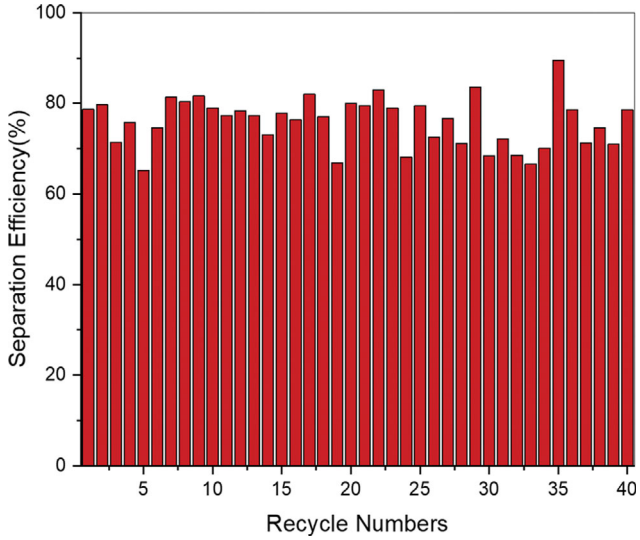

Fig. 6. Separation efficiency of hexane/water mixture using the highest efficient mesh.

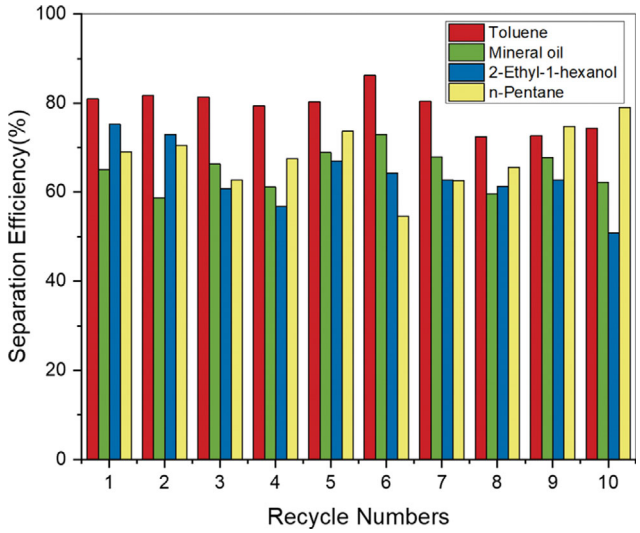

Fig. 7. Separation efficiency of different oil/water mixtures.

Another test, which helps to investigate how efficient the coating on the stainless-steel mesh, is the repeatability test. In this test, the most efficient coated mesh was used to separate the oil (hexane)/water mixture. The separation was repeated up to 40 times using the same mesh, and the separation efficiency was measured each time (Fig. 6). This test is very important since it will help to reduce the waste and the cost of the separation process. After repeating the separation of hexane/water mixture many times using the same coated mesh, the separation efficiency was still high (average 70%) and fast (a few seconds). This means that the coating is stable and can be used many times without losing its efficiency.

In addition, a stability test can also be performed to check if the coated mesh could separate different types of oil from water. In this test, different oils were used in the separation such as toluene, mineral oil, 2-ethyl-1-hexanol, and n-pentane. By looking at Fig. 7, one can notice that the coated mesh exhibits a separation efficiency above 60% for all four oil-water mixtures, which is quite good. The separation efficiency of different types of oil from water is still efficient even after repeating the separation ten times using the same mesh. In addition, the separation of all the oil-water mixture is fast. Not all the oils can be separated from water using this method, such as 1-pentanol, 1-butanol, and 2-propanol. These oils cannot be separated since they are mixed with water. Moreover, cooking oil cannot be separated using this method since it is highly viscous and will not pass through the mesh.

CONCLUSIONS

The nanostructured materials prepared were graphitic carbon nitride (g-C_3N_4) from different precursors. As-prepared g-C_3N_4 was immobilized on a stainless steel mesh to use as oil\water separating filter. The nature of the mesh can be determined from the contact angle measurements. All the uncoated meshes (with different mesh sizes) resulted in inefficient separation and allowed both water and oil to pass. After several tries, it was found that the most suitable mesh sizes were 50 μm and 75 μm, while the most suitable hydrophobic agent was HDTMS due to the long carbon chain in its structure. In addition, it was finally found that the most efficient and proper coating was g-C_3N_4 (precursor: thiosemicarbazide) functionalized with HDTMS, and it was coated on stainless steel mesh with 75 μm size. This coating resulted in fast separation in which it needs a few seconds to separate the oil/water mixture. In addition, the separation efficiency of this coated mesh reached 74.87%, which is quite good. It allowed the oil to pass completely through the mesh and blocked the passage of water (hydrophobic surface). Different tests were performed to study the properties of the most efficient coated mesh, such as repeatability, stability, and accuracy tests. From these tests, it was found that the coated mesh can be used up to 40 times under the same condition (Distilled water was colored using methylene blue (blue color), while the oil (toluene, hexane, mineral oil, 2-ethyl-1-hexanol, and n-pentane) was colored using Sudan red III (red color)) and still gave good efficiency. Moreover, it can separate different types of oil such as toluene, mineral oil, 2-ethyl-1-hexanol, and n-pentane and result in almost pure water with a very trace amount of oil.

ACKNOWLEDGEMENT

This research output was supported by Sultan Qaboos University and Qatar University for collaborative research funding project (CL/SQU-QU/SCI/20/01).

REFERENCES

1. H. Zhang, J. Qu, X. Fang, S. Lei, F. Wang, C. Li, W. Li, Y. Hu, A. Amirfazli and P. Wang, *Chem. Eng. J.*, **429**, 132539 (2022).
2. K. Li, W. Chen, W. Wu, Z. Pan, Z. Liang and J. Gan, *Prog. Org. Coat.*, **150**, 105979 (2021).
3. X. Q. Cheng, Y. Jiao, Z. Sun, X. Yang, Z. Cheng, Q. Bai, Y. Zhang, K. Wang and L. Shao, *ACS Nano*, **15**, 3500 (2021).
4. S. Jo and Y. Kim, *Korean J. Chem. Eng.*, **33**, 511 (2016).
5. Y. Wei, H. Qi, X. Gong and S. Zhao, *Adv. Mater. Interfaces*, **5**, 1800576

(2018).
6. X. Gong, Y. Wang, H. Zeng, M. Betti and L. Chen, *ACS Sustainable Chem. Eng.*, **7**, 11118 (2019).
7. C. Chen, D. Weng, A. Mahmood, S. Chen and J. Wang, *ACS Appl. Mater. Interfaces*, **11**, 11006 (2019).
8. R. Ghosh, R. P. Sahu, R. Ganguly, I. Zhitomirsky and I. K. Puri, *Ceram. Int.*, **46**, 3777 (2020).
9. H. Cai, Y. Mei, J. Chen, Z. Wu, L. Lan and D. Zhu, *J. Clean. Prod.*, **276**, 122783 (2020).
10. P. Adhikary, M. A. P. Mahmud, T. Solaiman and Z. L. Wang, *Nano Today*, **45**, 101513 (2022).
11. Y. Long, Y. Shen, H. Tian, Y. Yang, H. Feng and J. Li, *J. Membr. Sci.*, **565**, 85 (2018).
12. J.-J. Li, Y.-N. Zhou and Z.-H. Luo, *Prog. Polym. Sci.*, **87**, 1 (2018).
13. C. B. Agano, A. G. C. Villanueva, A. P. S. Cristobal, R. G. B. Madera, A. D. S. Montallana and M. R. Vasquez Jr., *Results Phys.*, **25**, 104257 (2021).
14. Y. Diao, M. Yan, X. Li, C. Zhou, B. Peng, H. Chen and H. Zhang, *Colloids Surf. A: Physicochem. Eng. Asp.*, **594**, 124511 (2020).
15. K. Ravichandran, K. Kalpana, M. M. Ibrahim and K. S. Seelan, *Mater. Today: Proc.*, **48**, 207 (2022).
16. F. A. Marzouqi, R. Selvaraj and Y. Kim, *Desalin. Water Treat.*, **116**, 267 (2018).
17. S. A. Mamari, F. A. Marzouqi, A. A. Nabhani, Y. Kim and R. Selvaraj, *Toxicol. Environ. Chem.*, **104**, 211 (2022).
18. F. Al Marzouqi, Y. Kim and R. Selvaraj, *Toxicol. Environ. New J. Chem.*, **43**(25), 9784 (2019).
19. F. Al Marzouqi and R. Selvaraj, *Catalysts*, **13**(3), 560 (2023).
20. F. Al Marzouqi, R. Selvaraj and Y. Kim, *Mater. Res. Express*, **6**(12), 125538 (2020).